Fabrication of large alumina foams by pyrolysis of thermo-foamed alumina–sucrose

Sujith Vijayan, Rajaram Narasimman, and Kuttan Prabhakaran[a)]
Department of Chemistry, Indian Institute of Space Science and Technology, Thiruvananthapuram, Kerala 695 547, India

(Received 21 July 2015; accepted 10 December 2015)

The aim of this study is to prevent cracks in large foam bodies prepared by thermo-foaming of alumina powder dispersions in molten sucrose. Cracks initiate in the binder burnout stage during which the bodies undergo shrinkage in the range of 32–49 vol% depending on sucrose content. Intermediate pyrolysis of the sucrose polymer binder prevents the cracking of large foam bodies as the carbon produced by pyrolysis binds the alumina particles during the initial stage of shrinkage and provides adequate strength to withstand the internal stresses produced during the pyrolysis and subsequent carbon burnout. The carbon bonded alumina foam bodies obtained after pyrolysis do not show any visible cracks during subsequent carbon burnout and sintering because the alumina particles establish a firm network with each other due to particle drag and rearrangement during pyrolysis of the sucrose polymer binder as evidenced from microstructure analysis. The carbon bonded alumina foam bodies show high compressive strength (2–1.3 MPa) and are amenable to machining operations such as milling and drilling without cracking.

I. INTRODUCTION

Ceramic foams are used in a variety of applications such as high temperature thermal insulation, molten metal filtration, catalyst support, lightweight structural components and preforms for polymer–ceramic and metal–ceramic composites.[1–5] Foaming and setting of ceramic powder suspensions, polymer foam replication, and emulsion templating are three well known methods for the preparation of ceramic foams. In the first method, foamed powder suspensions, produced by stabilizing gas bubbles with either surfactant or particles, are cast in a mold.[6–16] The cast foamed suspensions are then set by either in situ polymerization of organic monomers or by coagulation of the powder suspensions. The wet foam bodies are subsequently dried, binder removed, and sintered to produce the ceramic foams. In the second method, ceramic replica of a polymer foam template is produced by coating the polymer foam with a ceramic powder suspension followed by drying, burnout of the polymer foam template and sintering.[17–19] In the third method, a high internal phase emulsion is made by dispersing water immiscible liquid droplets in an aqueous ceramic powder suspension using an emulsifying agent. The emulsion cast in a mold is subsequently dried, oil removed, and sintered to produce ceramic foam.[20–23] Formation of cracks is likely during drying, binder removal, and sintering of large bodies.[24] Methods, such as water retention additives, freeze drying, and cross-linking of the polymeric binder, are used to prevent crack formation during drying of the wet-foams.[16,24]

Recently, we reported the thermo-foaming of powder dispersions in molten sucrose for the preparation of alumina foams.[25] The method produces interconnected cellular ceramics with porosity in the range of 94–93.3% at alumina powder to sucrose weight ratios in the range of 0.6–1.2.[25] The scanning electron microscopy (SEM) photomicrograph in Fig. 1 shows the typical cell structure of the alumina foam formed by thermo-foaming.[25] The process is eco-friendly as it does not use any synthetic organic additives. Moreover, the alumina foams produced have relatively high compressive strength (CS). Although the thermo-foaming process produces crack-free alumina foam bodies of smaller dimensions, attempts to fabricate large foam bodies resulted in severe cracking during sintering. In the present work, a two stage sintering strategy involving pyrolysis in inert atmosphere followed by carbon burnout and sintering in air was studied to produce large alumina foam bodies. The pyrolysis step not only prevents cracking of large foam bodies during sintering, but also increases the CS of the foamed body which enables green machining.

II. EXPERIMENTAL

α-Alumina powder (A16SG, ACC Alcoa, Kolkata, India) of 0.34 μm average particle size and specific

Contributing Editor: Gary L. Messing
[a)]Address all correspondence to this author.
e-mail: kp2952002@gmail.com
DOI: 10.1557/jmr.2015.395

surface area 10.4 m^2/g was used. Analytical reagent grade sucrose and acetone were procured from Merck India Ltd., Mumbai, India. The procedure for thermo-foaming of alumina powder dispersions in molten sucrose reported in our previous publication was adopted without modification.[25] Accordingly, a homogeneous mixture of sucrose (200 g) and alumina powder (160–240 g) was prepared by planetary ball milling and then heated at 185 °C in a 2.5 L borosilicate glass tray to melt the sucrose. The melt was stirred with a glass rod to uniformly mix the alumina powder in the molten sucrose. The alumina powder dispersion in the molten sucrose was heated for 24 h at 150 °C to form a sucrose polymer–alumina powder composite foam. The foam bodies were heated at 0.5 °C/min in an argon atmosphere at 900 °C and held for 2 h in an electrically heated box furnace to pyrolyze the sucrose and produce carbon bonded alumina foams. The samples were cooled under inert atmosphere to room temperature. The carbon bonded alumina foams were heated in air in an electrically heated sintering furnace up to 1600 °C for removal of the carbon and subsequent sintering. The heating rates used were 2 °C/min from room temperature to 400 °C, 0.5 °C/min from 400 to 600 °C and 2 °C/min from 600 to 1600 °C. Samples were sintered for 2 h at 1600 °C. The shrinkages of the foam bodies during pyrolysis, carbon burnout, and sintering were calculated from the dimensions.

Thermogravimetric analysis (TGA, Q-50, TA Instruments, New Castle, Delaware) of the sucrose polymer–alumina powder composite foams and carbon bonded alumina foam samples was carried out at 5 °C/min. The carbon content of carbon bonded alumina foam bodies was estimated by a gravimetric method. Carbon bonded alumina foam bodies of 5 cm × 5 cm × 2.5 cm were used for the estimation of carbon. The CSs of the sucrose polymer–alumina powder composite foams and carbon bonded alumina foams were measured according to the ASTM standard C365/C365-05 using rectangular samples of 25 mm × 25 mm × 12 mm size on a Universal Testing Machine (Instron 5984, Instron, Norwood, Massachusetts) at 0.5 mm/min. Machinability of the carbon bonded alumina foams was tested by milling slots and drilling holes in rectangular bodies using conventional machines and high speed steel tools.

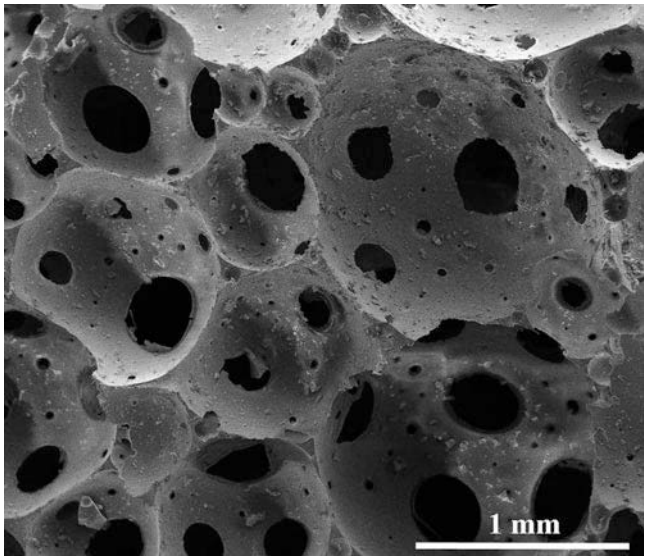

FIG. 1. Typical cell structure of alumina foam produced by thermo-foaming of powder dispersions in molten sucrose.

III. RESULTS AND DISUSSION

The direct heating of sucrose polymer–alumina powder composite foam bodies in air below 600 °C followed by sintering at 1600 °C resulted in severe cracking of samples larger than 5 cm × 5 cm × 2 cm while smaller bodies did not crack. Cracking of large foam bodies is believed to be due to the large shrinkage during the sintering stage. The total shrinkage observed during sintering of sucrose polymer–alumina powder composite foam bodies prepared at alumina powder to sucrose weight ratios of 0.6–1.2 ranged from 75.1 to 60 vol%.[25] The corresponding linear shrinkage is in the range of 39.1–29.1%. The shrinkage of the foam bodies mainly occurs in two stages. The first stage of shrinkage is during the sucrose polymer burnout at temperature below 600 °C and the second stage of shrinkage is during sintering at temperatures in the range of 1200–1600 °C. Figure 2 shows the total shrinkage and shrinkage during the sucrose polymer burnout as a function of alumina powder to sucrose weight ratio. The shrinkage during sucrose polymer burnout decreases from 49.2 to 31.7 vol% when the alumina powder to sucrose weight ratio increases from 0.6 to 1.2, respectively. The corresponding linear

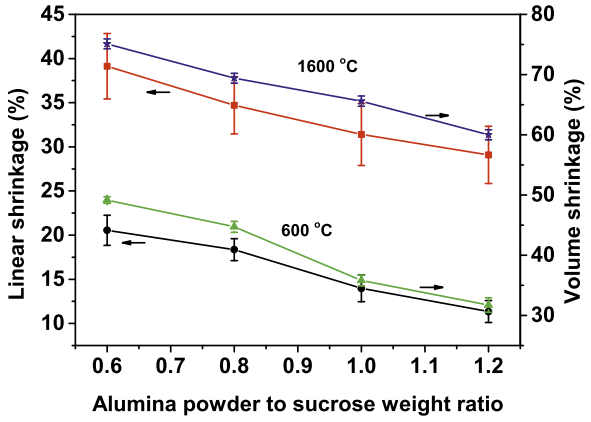

FIG. 2. Total shrinkage and shrinkage during polymer burnout of sucrose polymer–alumina powder composite foam bodies prepared at various alumina powder to sucrose weight ratio. (0.5 °C/min up to 600 °C with a dwell time of 2 h and 1 °C/min from 600 to 1600 °C with a dwell time of 2 h).

shrinkage observed is in the range of 20.5–11.3%, respectively. This shows that a majority of the volume shrinkage takes place during the sucrose polymer burnout.

It is well known that burnout of polymeric binder from ceramic green bodies containing a large amount of organic creates high strain which results in the development of internal stresses in the bodies. The stress–strain development during binder removal from ceramic green bodies is well studied by both experimental methods and mathematical modeling.[26–30] The magnitude of strain and stress developed during binder burnout depends on the nature and amount of binder. In the present case, the alumina powder–sucrose polymer composite foam bodies prepared at alumina powder to sucrose weight ratios in the range of 0.6–1.2 contain 56–38 wt% of sucrose polymer, respectively. The burnout of this large amount of polymer creates a linear strain in the range of 20.5–11.3% (volume shrinkage 49.2–31.7%). Moreover, large volumes of gases evolve due to thermal decomposition of the large amount of the sucrose polymer in the composite foam. In addition, during the thermal decomposition of the sucrose polymer binder, the strength of the cell walls and struts of the foams decreases. It appears that, at a certain stage, the internal stresses developed become higher than the strength of the struts and cell walls. At this stage, cracks originate in the foam bodies. The cracks that originate during the sucrose polymer burnout are aggravated during sintering at higher temperatures (Fig. S1, Supplementary material).

A way to alleviate the problem is to retain a binder phase during the first stage of shrinkage. Figure 3 shows the TGA graph in air and nitrogen atmosphere of sucrose polymer–alumina powder composite foam with an alumina powder to sucrose weight ratio of 0.6. The TGA in air atmosphere shows a weight loss of 56% at 525 °C corresponding to the complete burnout of the sucrose polymer. However, the TGA in nitrogen atmosphere shows a weight loss of only 39.8% up to 900 °C. The difference in weight loss in air and nitrogen atmosphere is because of the carbon retained due to the pyrolysis of the sucrose polymer. Calculations from the TGA results show that the sucrose polymer in the sucrose polymer–alumina powder composite foam retains 28.9 wt% of carbon during pyrolysis. This carbon produced from the sucrose polymer binds the alumina particles. That is, the heat treatment of sucrose polymer–alumina powder composite foams in inert atmosphere produces carbon bonded alumina foams. Gravimetric estimation shows the presence of 34–20 wt% carbon in carbon bonded alumina foam bodies obtained by pyrolysis of sucrose polymer–alumina powder composite foams prepared at alumina powder to sucrose weight ratios in the range of 0.6–1.2, respectively. The corresponding volume percentage (calculated by considering the density of carbon and alumina as 2.26 and 3.98 g/cm^3, respectively) of carbon in the carbon bonded alumina foams are in the range of 46.13–30.6. Interestingly, the shrinkage during pyrolysis of sucrose polymer–alumina powder composite foam bodies is more or less the same as that observed during the sucrose polymer burnout. This indicates that the carbon produced by pyrolysis of sucrose polymer just fills the voids present in the alumina particle assembly. The pyrolysis shrinkage and amount of carbon retained in the carbon bonded alumina foams are shown in Fig. 4. The large sucrose polymer–alumina powder composite foam bodies do not show any visible cracks during the pyrolysis. This indicates that the carbon produced binds the alumina particles and provides adequate strength to cell walls and struts to resist the formation of crack due to the internal stresses produced during the pyrolysis.

Figure 5 shows the TGA in air of a carbon bonded alumina foam sample with an alumina powder to sucrose weight ratio of 0.6. The sample shows a weight loss of

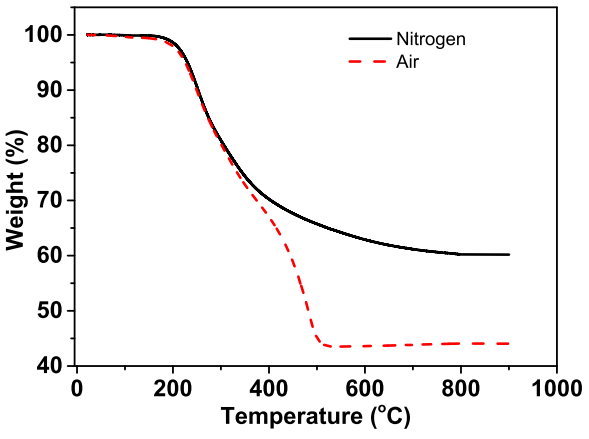

FIG. 3. TGA graph of sucrose polymer–alumina powder composite foam sample heated in air and nitrogen atmosphere (alumina powder to sucrose weight ratio is 0.6).

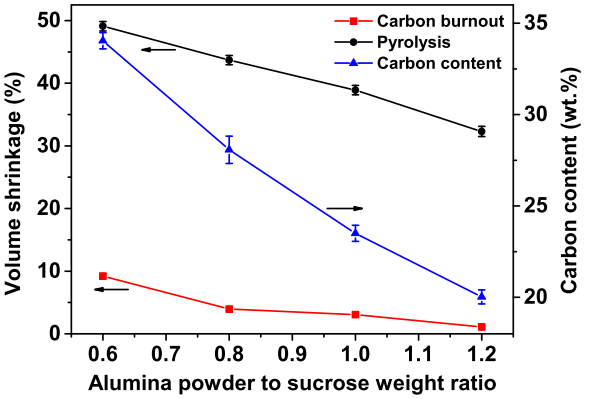

FIG. 4. Pyrolysis shrinkage, shrinkage during carbon burnout and carbon content in the carbon bonded alumina foam as a function of alumina powder to sucrose weight ratio (pyrolysis at 0.5 °C/min up to 900 °C with a dwell time of 2 h and carbon burnout at 1 °C/min up to 600 °C with a dwell time of 2 h).

only 2.5% up to 400 °C. The complete burnout of the carbon takes place between 400 and 600 °C. Therefore, a slow heating rate of 0.5 °C/min was used from 400 to 600 °C for carbon burnout of large bodies. The carbon bonded alumina foam bodies prepared at an alumina powder to sucrose weight ratio of 0.6 show a relatively high shrinkage of 9.2 vol% (linear shrinkage 3.7%, Fig. S2 Supplementary material) during the carbon burnout stage. However, at higher alumina powder to sucrose weight ratios, the shrinkage observed during carbon burnout is in the range of 3.9–1.1 vol% (linear shrinkage in the range of 1.24–0.34%) (Fig. 4). The large carbon bonded alumina foam bodies prepared at alumina powder to sucrose weight ratios in the range of 0.8–1.2 do not show any visible cracks during the carbon burnout stage as the internal strains are relatively low due to the low linear shrinkage of 1.24–0.34%. However, cracks are sometimes observed during carbon burnout from carbon bonded alumina large foam bodies prepared at an alumina powder to sucrose weight ratio of 0.6 due to the development of internal stresses as a result of the large shrinkage (9.23 vol%) during carbon burnout. Unlike the green alumina foams obtained after sucrose polymer burnout, the green alumina foams obtained after carbon burnout have very good stability against collapse during handling. Large green alumina foams of 18 cm × 10 cm × 2.5 cm after carbon burnout do not produce any visible crack during subsequent sintering (Fig. 6).

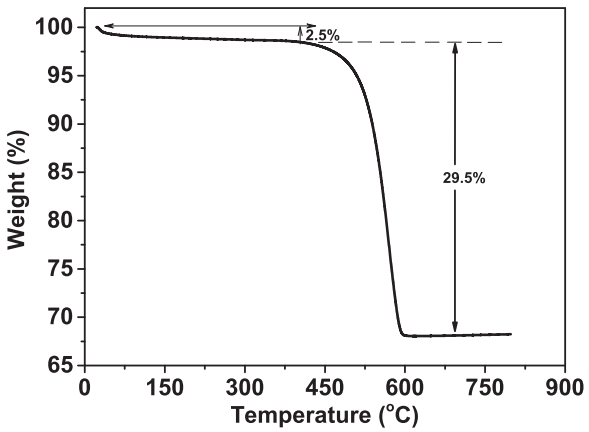

FIG. 5. TGA of a carbon bonded alumina foam sample heated in air at 5 °C/min (alumina powder to sucrose weight ratio is 0.6).

Microstructure changes during pyrolysis were studied by SEM. Figures 7(a) and 7(b) shows SEM photomicrographs of a fractured strut region of sucrose polymer–alumina powder composite foam and carbon bonded alumina foam at an alumina powder to sucrose weight ratio of 1. In the sucrose polymer–alumina powder composite foam, the alumina particles are embedded in a relatively thick sheath of the polymer matrix. On the other hand, in carbon bonded alumina foam, the alumina particles are bonded by a thin layer of carbon produced from the sucrose polymer. The shrinkage during the pyrolysis drags the alumina particles close to each other. It is also likely that the alumina particles undergo rearrangement to the more compact structure during polymer pyrolysis. This results in improved alumina particle packing. The improved alumina particle packing as a result of particle drag and rearrangement during polymer pyrolysis is clearly evidenced in the SEM photomicrograph of the alumina green foam obtained after carbon burnout from carbon bonded alumina foam. The SEM photomicrographs of the fractured strut region of alumina green foams obtained after polymer burnout from sucrose polymer–alumina powder composite foam and carbon burnout from carbon bonded alumina foam are shown in Figs. 7(c) and 7(d). It is interesting to note that the alumina green foam obtained after sucrose polymer burnout from sucrose polymer–alumina powder

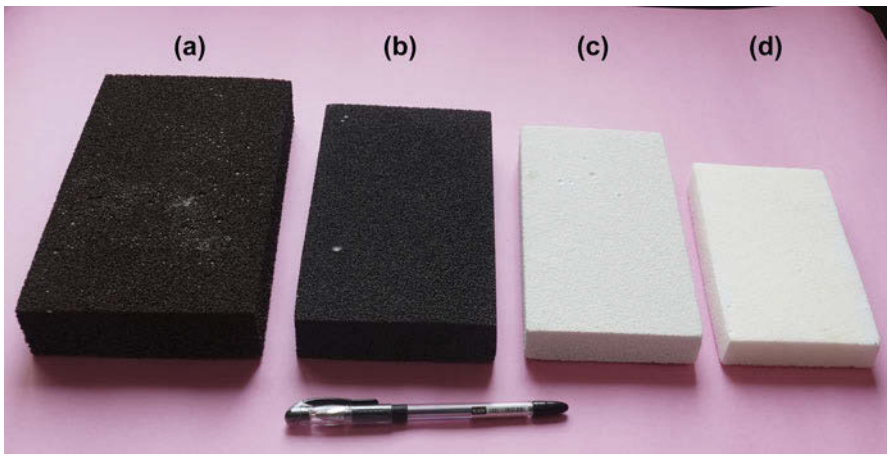

FIG. 6. Photograph showing large crack-free large alumina foam body prepared by the two stage sintering. (a) Sucrose polymer–alumina composite foam, (b) carbon bonded alumina foam, (c) alumina green foam after carbon burnout and (d) sintered alumina foam (alumina powder to sucrose weight ratio is 1).

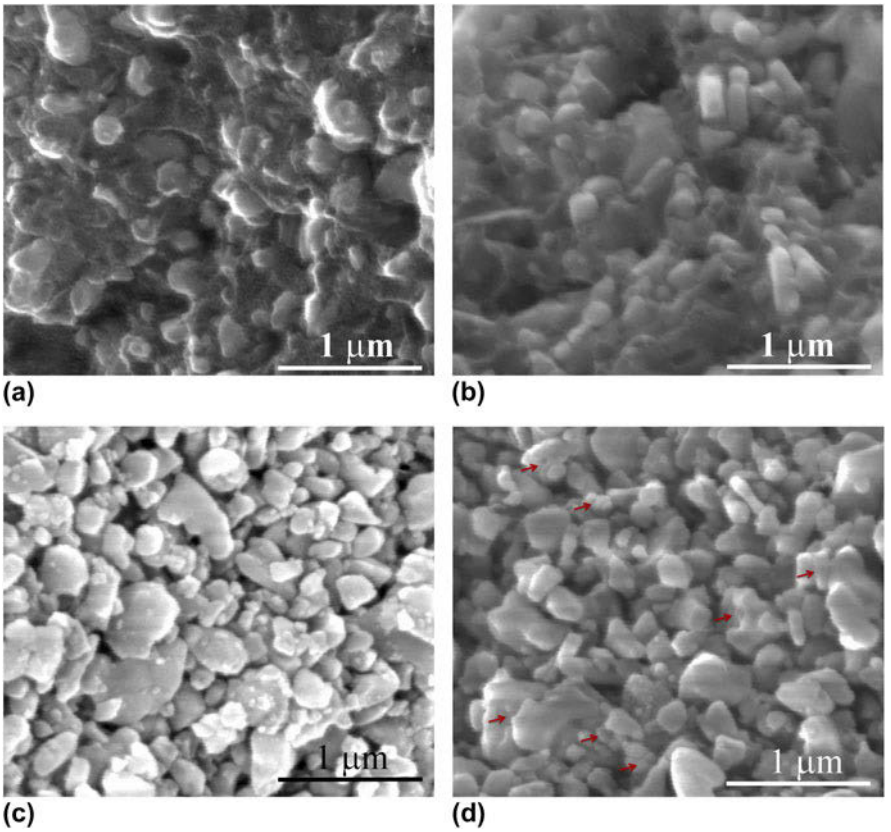

FIG. 7. High magnification SEM photomicrograph of fractured strut region of (a) sucrose polymer–alumina powder composite foam, (b) carbon bonded alumina foam, (c) green alumina foam after sucrose polymer burnout and (d) green alumina foam after carbon burnout prepared at an alumina powder to sucrose weight ratio of 1.

composite foam shows loosely packed alumina particles [Fig. 7(c)]. It appears that the alumina particles establish some weak bond with each other (may be the initiation of necking) during the pyrolysis at 900 °C. This is further evidenced by the fact that the large alumina green foam bodies obtained after carbon burnout from carbon bonded alumina foams have very good handling strength. In contrast, the alumina green foams obtained by sucrose polymer burnout from sucrose polymer–alumina powder composite foams are highly fragile to handle. It is interesting to note that the introduction of an additional pyrolysis step does not produce much variation in the final porosity of the sintered alumina foams. That is, the porosity remains in the same range of 93.3–94%.[25]

Green machining is an important aspect in ceramic processing as the machining of sintered bodies to produce ceramic components with required size and contour is very difficult.[31–34] Though the machining of dense green bodies obtained by gelcasting and powder pressing is widely studied, the green machining of ceramic foams is rarely reported.[35–38] The requirements for green machining are (i) the green foam should have sufficient strength to be held in the conventional lathe, milling machine and drilling machine, (ii) the machined surfaces should have very good finish and (iii) the green machining should not induce any cracks during the subsequent sintering. Figure 8 shows the CS and Young's modulus (YM) of sucrose polymer–alumina powder composite foams and carbon bonded alumina foams as a function of alumina powder to sucrose weight ratio. The CS and YM of sucrose polymer–alumina powder composite foams show a marginal increase from 0.6 to 0.9 MPa and 16 to 40 MPa, respectively, when the alumina powder to sucrose weight ratio increases from 0.6 to 1.2, respectively. The particle packing in struts and cell walls of alumina powder-sucrose polymer composite foam bodies depends on the alumina powder to sucrose weight ratio. At lower alumina powder to sucrose weight ratios, the sucrose polymer forms a thick layer around the alumina particles which prevents close packing of alumina particles. The thickness of the sucrose polymer layer decreases with an increase in alumina powder to sucrose weight ratio that leads to improved particle packing. The increase in CS and YM in spite of a decrease in sucrose polymer content (from 56 to 38 wt%) indicates that the increase in CS and YM with an increase in alumina powder to sucrose weight ratio is due to the increase in particle packing in the strut and cell walls of the foam.

There is a considerable improvement in the CS upon pyrolysis. In contrast to the sucrose polymer–alumina powder composite foams, the CS of carbon bonded alumina foams decreases from 2.06 to 1.3 MPa when the alumina powder to sucrose weight ratio increases from 0.6 to 1.2. The corresponding decrease in YM is from 75.2 to 38.2 MPa, respectively. It is well known that the strength of brittle cellular foams depends on its porosity, cell size, and strut thickness.[39–41] In general, the CS and YM of a brittle foam decrease when the porosity and cell size increase and strut thickness decreases. In the present case, the CS and YM depend also on the amount of carbon which binds the alumina particles. The bulk density of carbon bonded alumina foams decreases from 0.274 to 0.259 g/cm^3 when the alumina powder to sucrose weight ratio increases from 0.6 to 1.2, respectively. The porosity of the carbon bonded alumina foams calculated by considering the theoretical density of alumina (3.98 g/cm^3) and graphite (2.26 g/cm^3) shows a marginal increase from 91.25 to 92.48 vol%. However, we have observed an increase in cell size and strut thickness with an increase in alumina powder to sucrose weight ratio from 0.6 to 1.2.[25] The decrease in CS and YM with an increase in alumina powder to sucrose weight ratio can be attributed to the decrease in carbon content which binds the alumina particles, an increase in porosity, and an increase in cell size.

The CS of sucrose polymer–alumina powder composite foams is sufficient for their easy handling and light machining with an emery paper. The possibility of light machining in green foam is reported in the literature.[38] However, our attempt to machine samples by holding them in a milling machine and a drilling machine results in severe damage to the foam bodies. On the other hand, the strength of the carbon bonded alumina foams is sufficiently high to be held in either a milling or drilling machine without any damage. A photograph of a rectangular carbon bonded alumina foam body revealing slots made by milling using a conventional high speed steel tool is shown in Fig. 9. The green machined surface shows very good finish. Moreover, sharp edges and corners can be produced

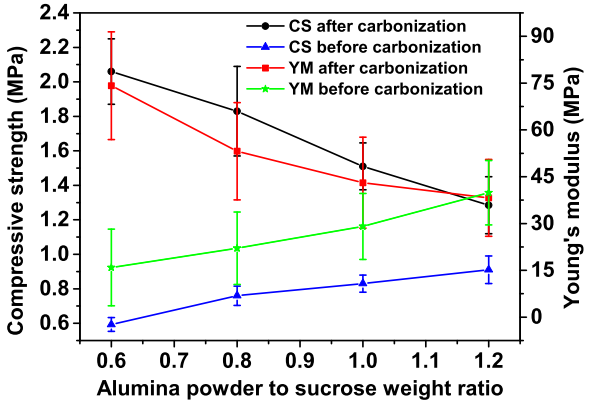

FIG. 8. CS and YM of sucrose polymer–alumina powder composite foams and carbon bonded alumina foams as a function of alumina powder to sucrose weight ratio.

FIG. 9. Photograph showing slots made by milling a rectangular carbon bonded alumina foam body in a conventional milling machine using a high speed steel tool.

FIG. 10. Photograph of alumina foam bodies prepared by carbon burnout and sintering of green machined carbon bonded alumina foam bodies. The slots are made by milling and holes are made by drilling.

by the green machining of carbon bonded alumina foams. The green machined carbon bonded alumina foam bodies prepared at alumina powder to sucrose weight ratios in the range of 0.8–1.2 do not show any visible cracks during the subsequent carbon burnout and sintering. Figure 10 shows a photograph of sintered alumina ceramic foams prepared by carbon burnout and sintering of the green machined carbon bonded alumina foams showing the slots made by milling and holes made by drilling.

IV. CONCLUSION

Direct binder burnout followed by sintering of large precursor foam bodies produced by thermo-foaming of alumina powder dispersions in molten sucrose resulted in severe cracking. The cracks are initiated during the binder removal stage due to the development of internal stresses as a result of the large strains (22.45–11.35%) corresponding to volume shrinkages observed in the range of 49–32%. Pyrolysis of the sucrose polymer binder before sintering in air atmosphere prevents sintering cracks in large foam bodies. The carbon produced from the sucrose polymer binds the alumina particles during the initial stage of shrinkage and increases the strength of cell walls and struts that resist cracking. The drag and rearrangement of alumina particles during pyrolysis lead to solid contacts and network between alumina particles as evidenced from microstructure analysis. The carbon bonded alumina foam bodies have relatively high CS and are amenable to machining in the green state using conventional tools. The machining does not induce any visible cracks during subsequent carbon burnout and sintering.

ACKNOWLEDGMENTS

The authors are thankful to Dr. K.S. Dasgupta, Director and Dr. Kuruvilla Joseph, Head of the Department of Chemistry of IIST for their encouragements.

REFERENCES

1. J. Saggio-Woyansky and C.E. Scott: Processing of porous ceramics. *Am. Ceram. Soc. Bull.* **71**, 1674 (1992).
2. M. Takahashi, R.L. Menchavez, M. Fuji, and H. Takegami: Opportunities of porousceramics fabricated by gelcasting in mitigating environmental issues. *J. Eur. Ceram. Soc.* **29**, 823 (2009).
3. J. Binner, H. Chang, and R. Higginson: Processing of ceramic–metal interpenetrating composites. *J. Eur. Ceram. Soc.* **29**, 837 (2009).
4. H. Haugen, J. Will, A. Köhler, U. Hopfner, J. Aigner, and E. Wintermantel: Ceramic TiO_2-foams: Characterisation of a potential scaffold. *J. Eur. Ceram. Soc.* **24**, 661 (2004).
5. R. Faure, F. Rossignol, T. Chartier, C. Bonhomme, A. Maître, G. Etchegoyen, P.D. Gallo, and D. Gary: Alumina foam catalyst supports for industrial steam reforming processes. *J. Eur. Ceram. Soc.* **31**, 303 (2011).
6. P. Sepulveda: Gelcasting of foams for porous ceramics. *Am. Ceram. Soc. Bull.* **76**, 61 (1997).
7. P. Sepulveda and J.G.P. Binner: Processing of cellular ceramics by foaming and *in situ* polymerization of organic monomers. *J. Eur. Ceram. Soc.* **19**, 2059 (1999).
8. J.G.P. Binner: Production and properties of low density engineering ceramic foam. *Br. Ceram. Trans.* **96**, 247 (1997).
9. X. Mao, S. Shimai, and S. Wang: Gelcasting of alumina foams consolidated by epoxy resin. *J. Eur. Ceram. Soc.* **28**, 217 (2008).
10. F.S. Ortega, P. Sepulveda, and V.C. Pandolfelli: Monomer systems for the gel-casting of foams. *J. Eur. Ceram. Soc.* **22**, 1395 (2002).
11. F.S. Ortega, F.A.O. Valenzuela, C.H. Scuracchio, and V.C. Pandolfelli: Alternative gelling agents for the gelcasting of ceramic foams. *J. Eur. Ceram. Soc.* **23**, 75 (2003).
12. I. Garrn, C. Reetz, N. Brandes, L.W. Kroh, and H. Schubert: Clot-forming: The use of proteins as binders for producing ceramic foams. *J. Eur. Ceram. Soc.* **24**, 579 (2004).
13. B.P. Binks and T.S. Horozov: Aqueous foams stabilized solely by silica nanoparticles. *Angew. Chem., Int. Ed.* **44**, 3722 (2005).
14. U.T. Gonzenbach, A.R. Studart, E. Tervoort, and L.J. Gauckler: Ultra stable particle-stabilized foams. *Angew. Chem., Int. Ed.* **45**, 3526 (2006).
15. A.R. Studart, U.T. Gonzenbach, E. Tervoort, and L.J. Gauckler: Processing routes to macroporous ceramics: A review. *J. Am. Ceram. Soc.* **89**, 1771 (2006).
16. U.T. Gonzenbach, A.R. Studart, D. Steinlin, E. Tervoort, and L.J. Gauckler: Processing of particle-stabilized wet foams into porous ceramics. *J. Am. Ceram. Soc.* **90**, 3407 (2007).
17. K. Schwartzwalder and A.V. Somers: Method of making porous ceramic article. U.S. Patent No 3 090 094, May 21, 1963.
18. J.W. Brockmeyer: Process for preparing ceramic foam. U.S. Patent No 4610 832, September 9, 1986.
19. X.W. Zhu, D.L. Jiang, and S.H. Tan: Impregnating process of reticulated porous ceramics using polymeric sponge as template. *J. Inorg. Mater.* **16**, 1144 (2001).
20. S. Barg, E.G. de Moraes, D. Koch, and G. Grathwohl: New cellular ceramics from high alkane phase emulsified suspensions (HAPES). *J. Eur. Ceram. Soc.* **29**, 2439 (2009).
21. E.M.M. Ewais, S. Barg, G. Grathwohl, A.A. Garamoon, and N.N. Morgan: Processing of open porous zirconia via alkane-phase emulsified suspensions for plasma applications. *Int. J. Appl. Ceram. Tech.* **8**, 85 (2011).
22. M.A. Alves-Rosa, L. Martins, S.H. Pulcinelli, and C.V. Santilli: Design of microstructure of zirconia foams from the emulsion template properties. *Soft Matter* **9**, 550 (2013).
23. S. Vijayan, R. Narasimman, and K. Prabhakaran: Freeze gelcasting of hydrogenated vegetable oil-in-aqueous alumina slurry emulsions for the preparation of macroporous ceramics. *J. Eur. Ceram. Soc.* **34**, 4347 (2014).
24. C. Chuanuwatanakul, C. Tallon, D.E. Dunstan, and G.V. Franks: Producing large complex-shaped ceramic particle stabilized foams. *J. Am. Ceram. Soc.* **96**, 1407 (2013).
25. S. Vijayan, R. Narasimman, C. Prudvi, and K. Prabhakaran: Preparation of alumina foams by the thermo-foaming of powder dispersions in molten sucrose. *J. Eur. Ceram. Soc.* **34**, 425 (2014).
26. Z.C. Feng, B. He, and S.J. Lombardo: Stress distribution in porous ceramic bodies during binder burnout. *J. Appl. Mech.* **69**, 497 (2002).
27. D.S. Tsai: Pressure buildup and internal stresses during binder burnout: Numerical analysis. *AIChE J.* **37**, 547 (1991).
28. W.J. Tseng and C. Hsu: Cracking defect and porosity evolution during thermal debinding in ceramic injection moldings. *Ceram. Int.* **25**, 461 (1999).

29. A. Maxirnenko and O.V. Biest: Finite element modeling of binder removal from ceramic mouldings. *J. Eur. Cer. Soc.* **18**, 1001 (1998).
30. Y.C. Lam, S.C.M. Yu, K.C. Tam, and Y. Shengjie: Simulation of polymer removal from a powder injection molding compact by thermal debinding. *Metall. Mater. Trans. A* **31**, 2597 (2000).
31. B. Su, S. Dhara, and L. Wang: Green ceramic machining: A top-down approach for the rapid fabrication of complex-shaped ceramics. *J. Eur. Ceram. Soc.* **28**, 2109 (2008).
32. F. Filser, P. Kocher, and L.J. Gauckler: Net-shaping of ceramic components by direct ceramic machining. *Assemb. Autom.* **23**, 382 (2003).
33. N.D. Butler, D.J. Dawson, and R.A. Wordsworth: Shaping complex components by green machining. *Proc. Br. Ceram. Soc.* **45**, 53 (1990).
34. S.D. Nunn and G.H. Kirby: Green machining of gelcast ceramic materials. *Ceram. Eng. Sci. Proc.* **17**, 209 (1996).
35. S. Dhara and B. Su: Green machining to net shape alumina ceramics prepared using different processing routes. *Int. J. Appl. Ceram. Tech.* **2**, 262 (2005).
36. K. Prabhakaran, C. Pavithran, M. Brahmakumar, and S. Ananthakumar: Gelcasting of alumina using urea-formaldehyde III. Machinable green bodies by co-polymerization with acrylic acid. *Ceram. Int.* **27**, 185 (2001).
37. X.L.K. Wu and W.J. McAnany: Acrylic binder for green machining. *Am. Ceram. Soc. Bull.* **75**, 61 (1995).
38. S. Dhara and P. Bhargava: A simple direct casting route to ceramic foams. *J. Am. Ceram. Soc.* **86**, 1645 (2003).
39. L.J. Gibson and M.F. Ashby: *Cellular Solids: Structure and Properties*, 2nd ed. (Cambridge University Press, Cambridge, England, 1997); pp. 175–234.
40. J. Verma, R. Mitra, and M. Vijayakumar: Processing of silica foam using steam heating and its characterization. *J. Eur. Ceram. Soc.* **33**, 943 (2013).
41. F.A. Costa Oliveira, S.M. Dias. M. Fatima Vaz, and J. Cruz Fernandes: Behaviour of open-cell cordierite foams under compression. *J. Eur. Ceram. Soc.* **26**, 179 (2006).

Supplementary Material

To view supplementary material for this article, please visit http://dx.doi.org/jmr.2015.395.